Radboud Universiteit

GRAPHENE FLAGSHIP

Many-body effects in graphene

Mikhail Katsnelson

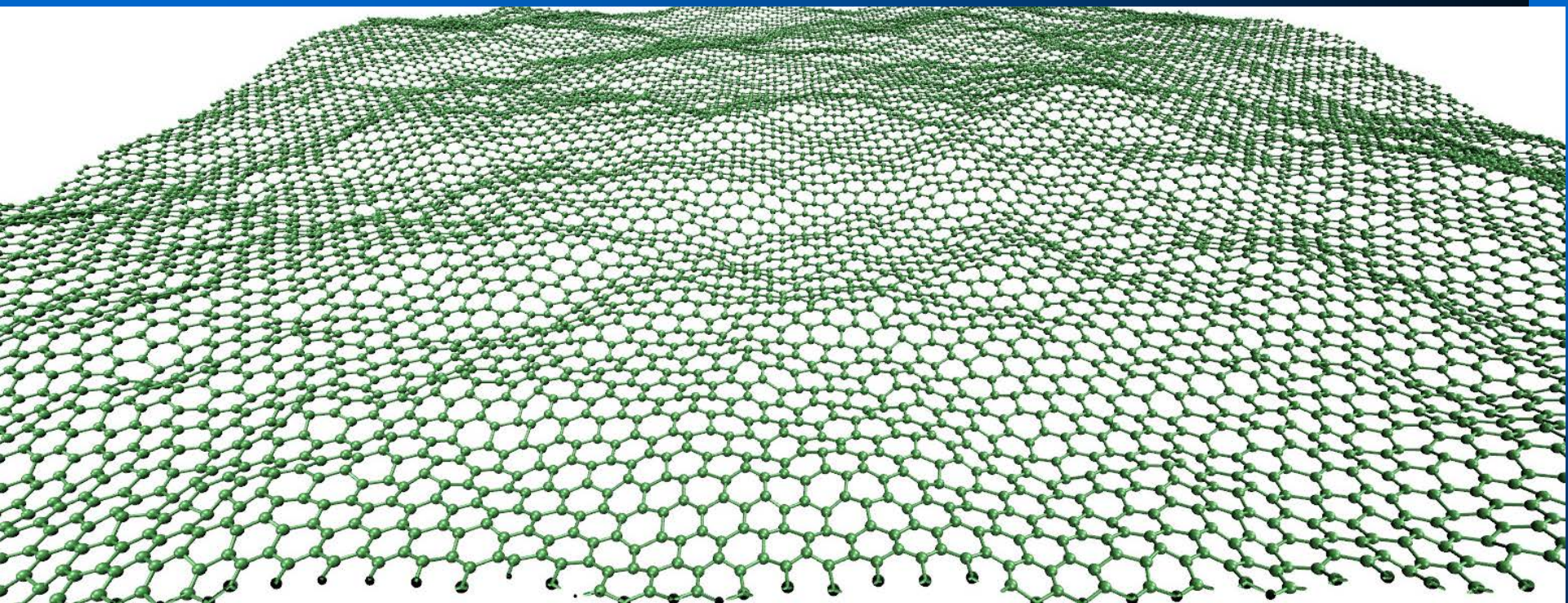

Outline

Introduction: Graphene and massless Dirac fermions

Realistic interelectron interactions in graphene: mapping on pi-band and on effective Hubbard model

Is freely suspended graphene semimetal or excitonic insulator?

Screening and optical properties

Non-Fermi-liquid behavior in weak interaction regime

Many-body renormalization of ballistic conductivity at the neutrality point

Carbon, an elemental solid

Diamond

Graphite

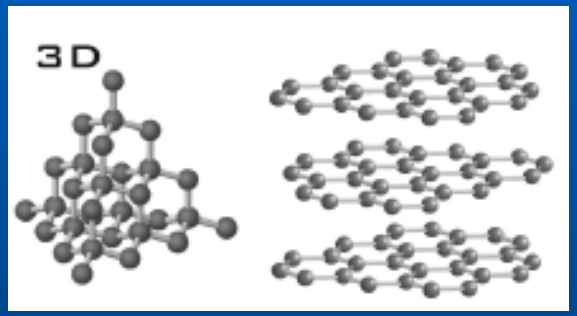

Crystal lattices

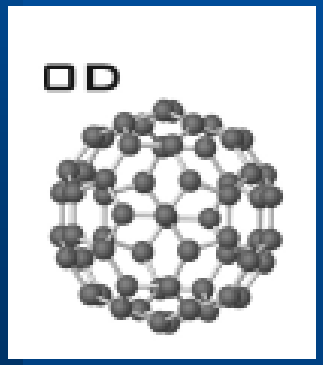

Fullerenes

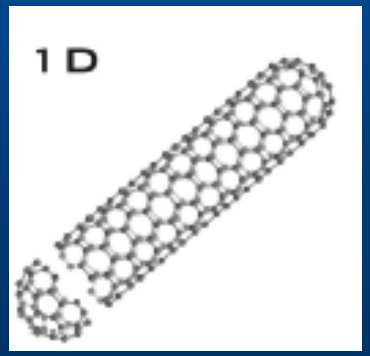

Nanotubes

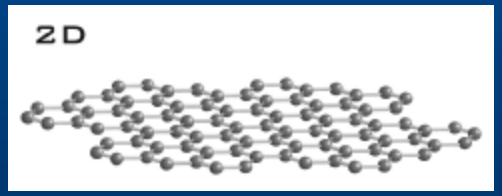

Graphene

Mother of all graphitic forms

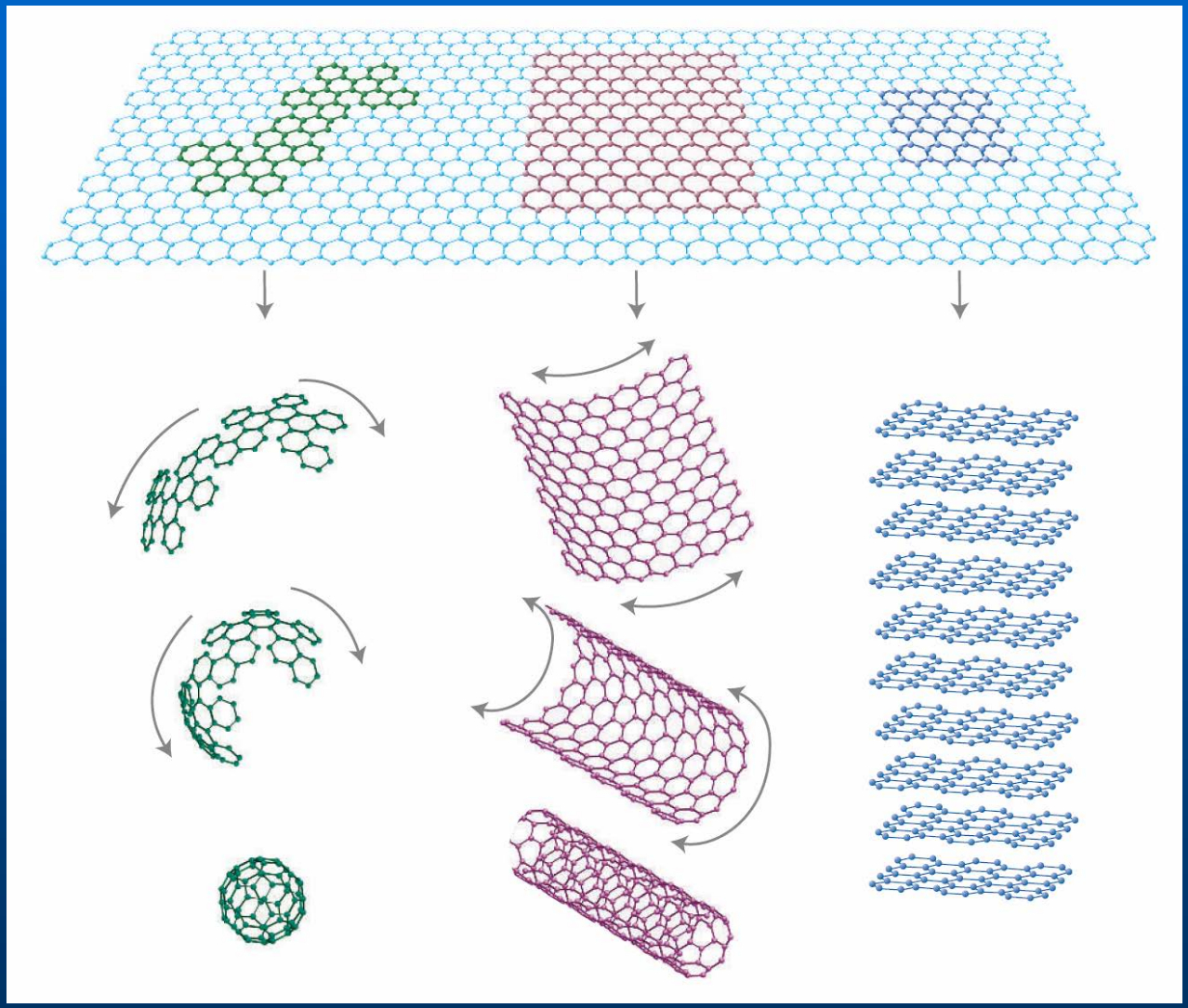

Fullerenes Nanotubes Graphite

Why graphene is interesting?

Till 2004: a way to understand graphite, nanotubes, fullerenes + theoretical interest
(Dirac point Wallace 1947, McClure 1956…)

Do we theoreticians need experimentalists?! – Yes!!!
(Klein tunneling, supercritical charge, ripples, new wave equation – bilayer, new type of transport…)

1. *Applications (modern electronics is 2D, bulk is ballast)*
2. *Prototype membrane (new drosophila for 2D statistical mechanics)*
3. *CERN on the desk (mimic high energy physics)*

Honeycomb lattice

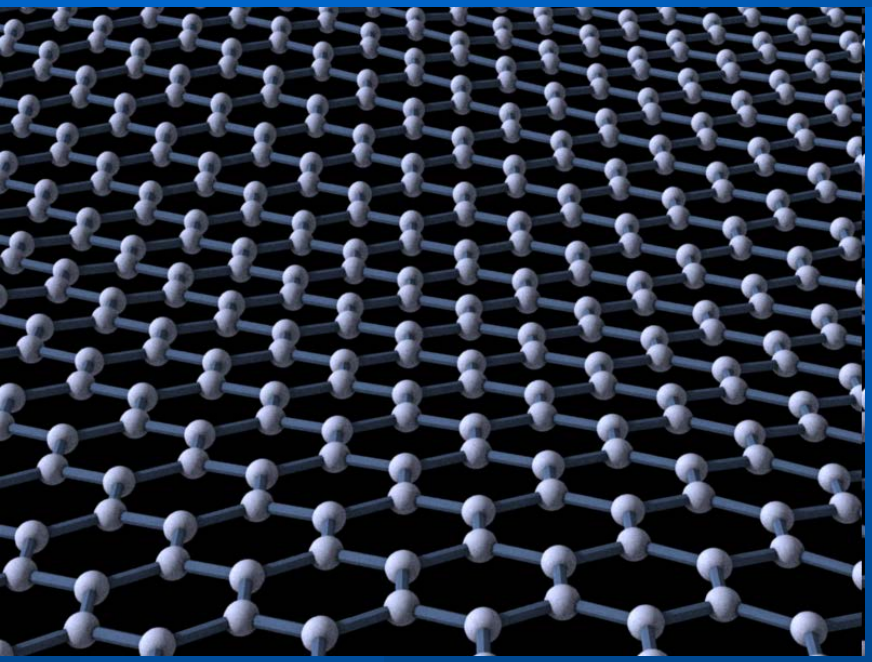

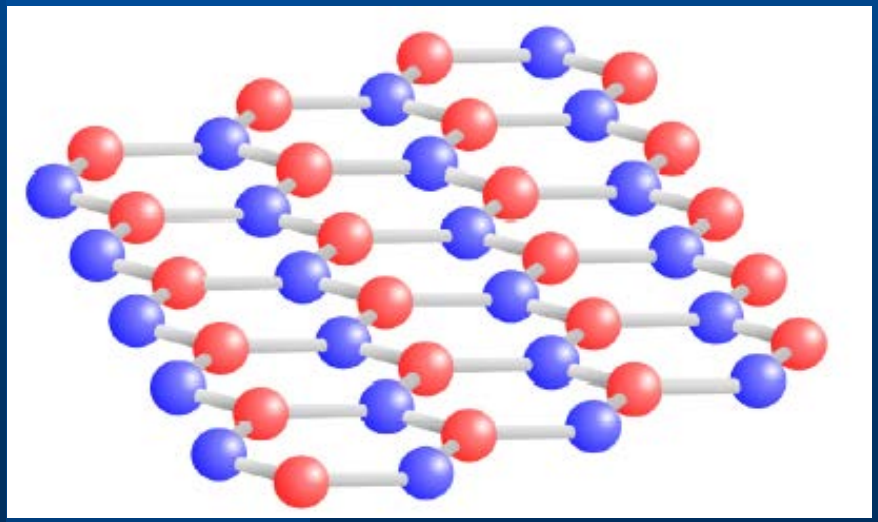

Two equivalent sublattices, A and B (pseudospin)

Massless Dirac fermions

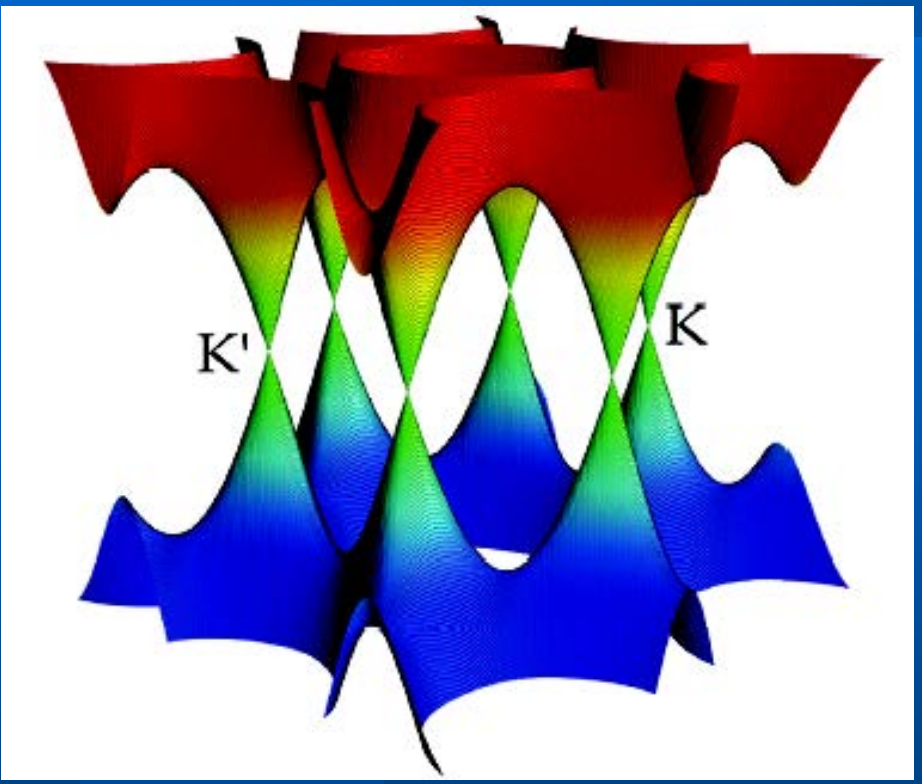

sp^2 hybridization, π bands crossing the neutrality point

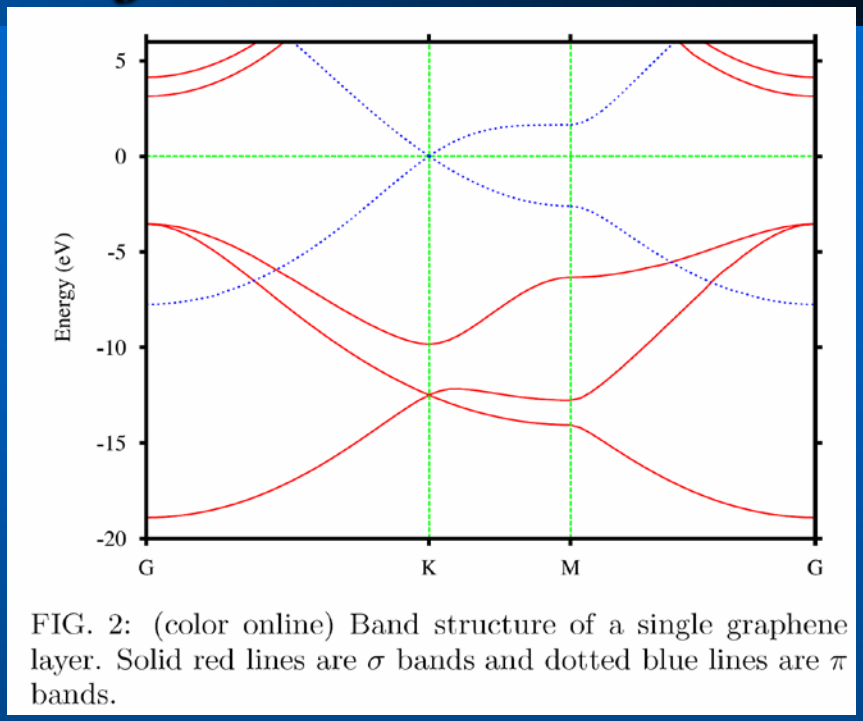

FIG. 2: (color online) Band structure of a single graphene layer. Solid red lines are σ bands and dotted blue lines are π bands.

Neglecting intervalley scattering: massless Dirac fermions

Massless relativistic particles (light cones)

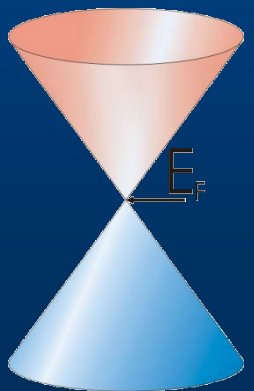

Symmetry protected (*T* and *I*)

Massless Dirac fermions II

Spectrum near *K* (*K'*) points is linear.
Conical cross-points: provided by symmetry and thus robust property

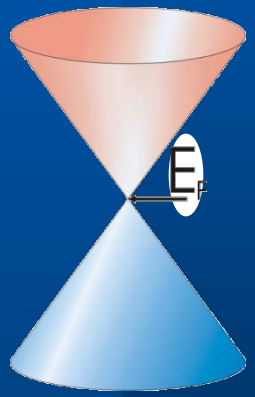

Undoped

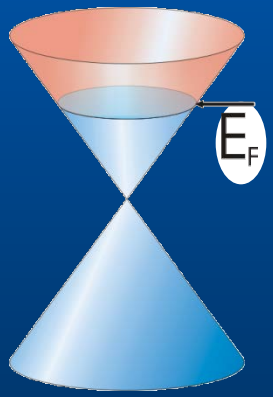

Electron

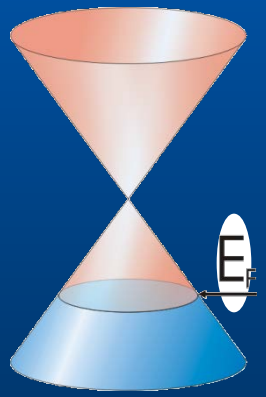

Hole

Massless Dirac fermions III

If Umklapp-processes K-K’ are neglected:
2D Dirac massless fermions with the Hamiltonian

$$H = -i\hbar c^* \begin{pmatrix} 0 & \dfrac{\partial}{\partial x} - i\dfrac{\partial}{\partial y} \\ \dfrac{\partial}{\partial x} + i\dfrac{\partial}{\partial y} & 0 \end{pmatrix} \qquad \hbar c^* = \frac{\sqrt{3}}{2}\gamma_0 a$$

“Spin indices’’ label sublattices *A* and *B*
rather than real spin

Massless Dirac fermions in condensed matter physics

1. d-wave superconductors
2. Vortices in superconductors and in superfluid helium-3
3. Topological insulators
4. Graphene

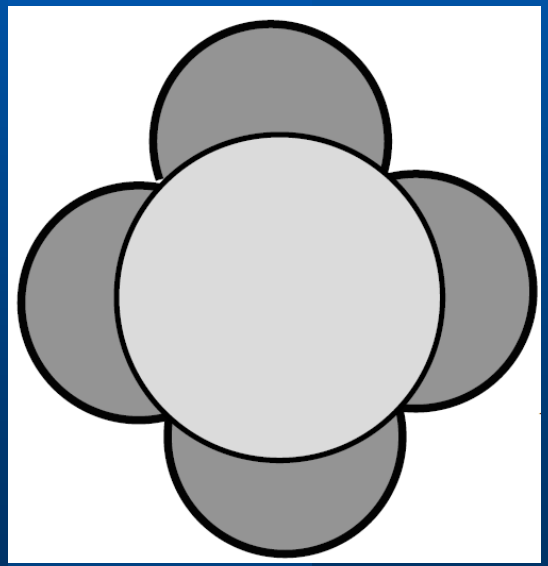

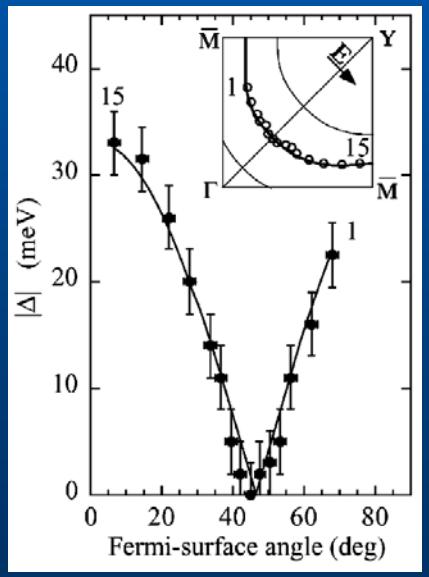

Gap in high-Tc cuprates

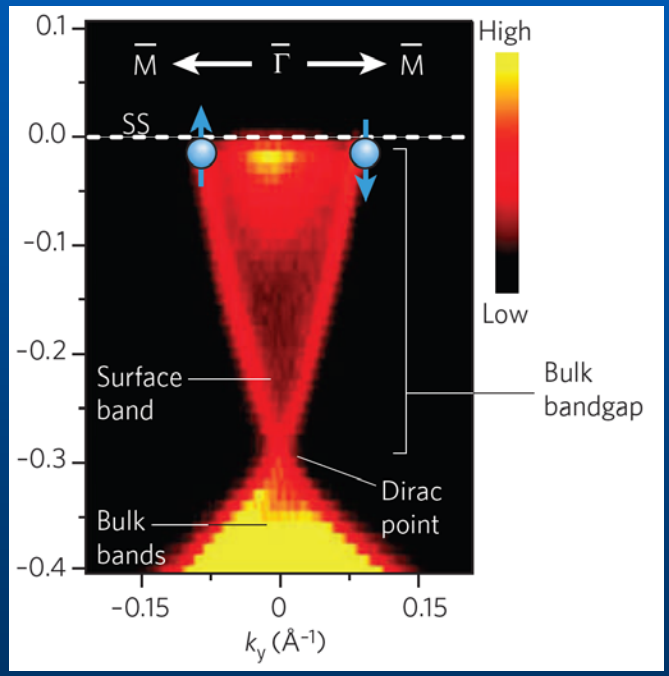

Electronic structure on surface of Bi_2Se_3

Strength of Coulomb interactions in graphene

Wehling, Şaşıoğlu, Friedrich, Lichtenstein, MIK & Blügel, PRL106, 236805 (2011

Generalized Hubbard model for π-bands only

$$\hat{H}_0 = -t \sum_{\langle \mathbf{i},\mathbf{j}\rangle,\sigma} c^{\dagger}_{\mathbf{i},\sigma} c_{\mathbf{j},\sigma} - t' \sum_{\ll \mathbf{i},\mathbf{j}\gg,\sigma} c^{\dagger}_{\mathbf{i},\sigma} c_{\mathbf{j},\sigma}$$

$$+U_{00} \sum_{\mathbf{i}} n_{\mathbf{i},\uparrow} n_{\mathbf{i},\downarrow} + \frac{1}{2} \sum_{\mathbf{i}\neq\mathbf{j},\sigma,\sigma'} U_{\mathbf{ij}} n_{\mathbf{i},\sigma} n_{\mathbf{j},\sigma'}$$

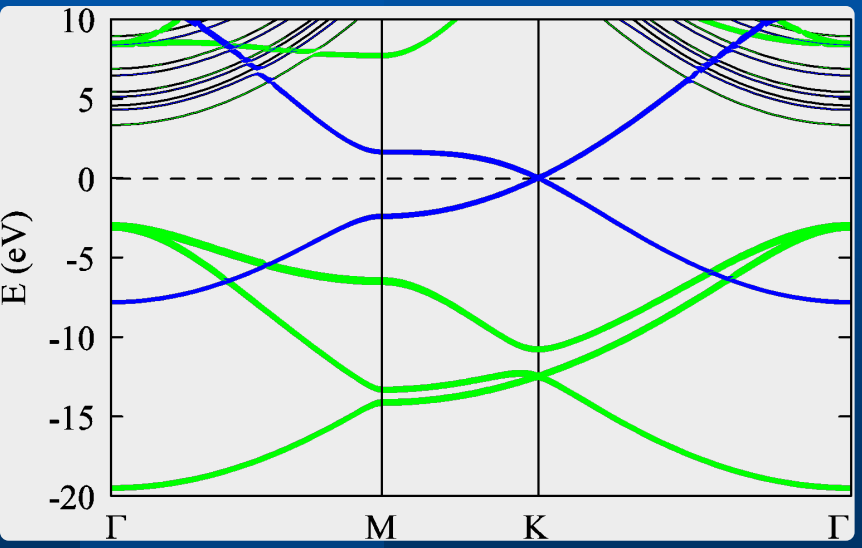

π bands (blue) crossing Fermi level

σ bands (green) at higher energies

All electrons except π contribute to screening of the Coulomb interactions (constrained RPA)

$$P(\mathbf{r},\mathbf{r}';\omega) = \sum_{i}^{\text{occ}} \sum_{j}^{\text{unocc}} \psi_i(\mathbf{r})\psi_i^*(\mathbf{r}')\psi_j^*(\mathbf{r})\psi_j(\mathbf{r}') \times \left\{ \frac{1}{\omega - \varepsilon_j + \varepsilon_i + i0^+} - \frac{1}{\omega + \varepsilon_j - \varepsilon_i - i0^+} \right\}$$

Polarization function

Strength of Coulomb interactions in graphene II

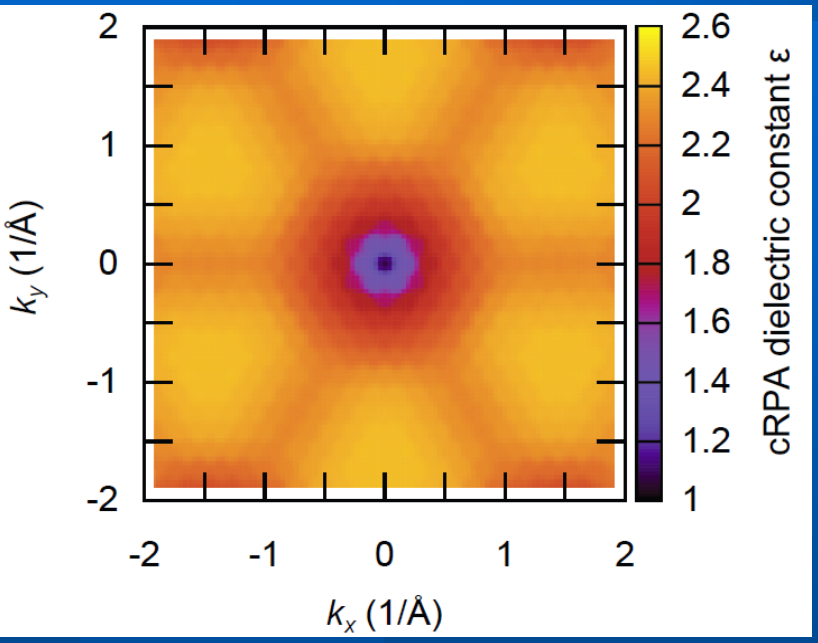

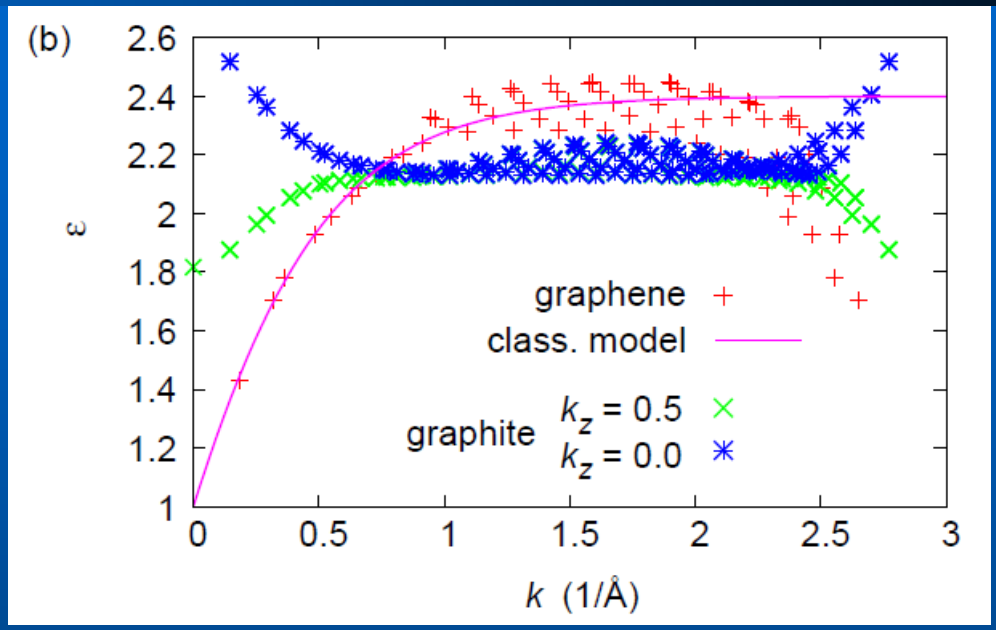

Static cRPA dielectric function of graphene in momentum space

Graphene vs graphite

	graphene		graphite	
	bare	cRPA	bare	cRPA
U_{00}^{A} (eV)	17.0	9.3	17.5	8.0
U_{00}^{B} (eV)	17.0	9.3	17.7	8.1
U_{01} (eV)	8.5	5.5	8.6	3.9

Effective Hubbard model for graphene

Schűler, Rösner, Wehling, Lichtenstein & MIK, PRL 111, 036601 (2013)

Long-range Coulomb interection is crucially important for graphene but not everywhere, e.g., for magnetism effective Hubbard model should be OK. How to build it?

We have:

$$H = -\sum_{i,j,\sigma} t_{ij} c^{\dagger}_{i\sigma} c_{j\sigma} + U \sum_{i} n_{i\uparrow} n_{i\downarrow} + \frac{1}{2} \sum_{\substack{i \neq j \\ \sigma,\sigma'}} V_{ij} n_{i\sigma} n_{j\sigma'}$$

We want:

$$H^* = -\sum_{i,j,\sigma} t_{ij} c^{\dagger}_{i\sigma} c_{j\sigma} + U^* \sum_{i} n_{i\uparrow} n_{i\downarrow}$$

Effective Hubbard model for graphene II

The idea: Feynman-Peirels-Bogoliubov variational principle

$$\tilde{\Phi}[\rho^*] = \Phi^* + \langle H - H^* \rangle^*$$

$$\Phi^* = -\frac{1}{\beta} \ln Z^*$$

$$\rho^* = 1/Z^* e^{-\beta H^*}$$

$$Z^* = \mathrm{Tr}\left\{ e^{-\beta H^*} \right\}$$

$\langle \dots \rangle^*$ denotes the Gibbs average over the trial system

$$\partial_{U^*} \tilde{\Phi}[U^*] = 0$$

$$U^* = U + \frac{1}{2} \sum_{\substack{i \neq j \\ \sigma, \sigma'}} V_{ij} \frac{\partial_{U^*} \langle n_{i\sigma} n_{j\sigma'} \rangle^*}{\sum_l \partial_{U^*} \langle n_{l\uparrow} n_{l\downarrow} \rangle^*}$$

The calculations are done by lattice QMC

Effective Hubbard model for graphene III

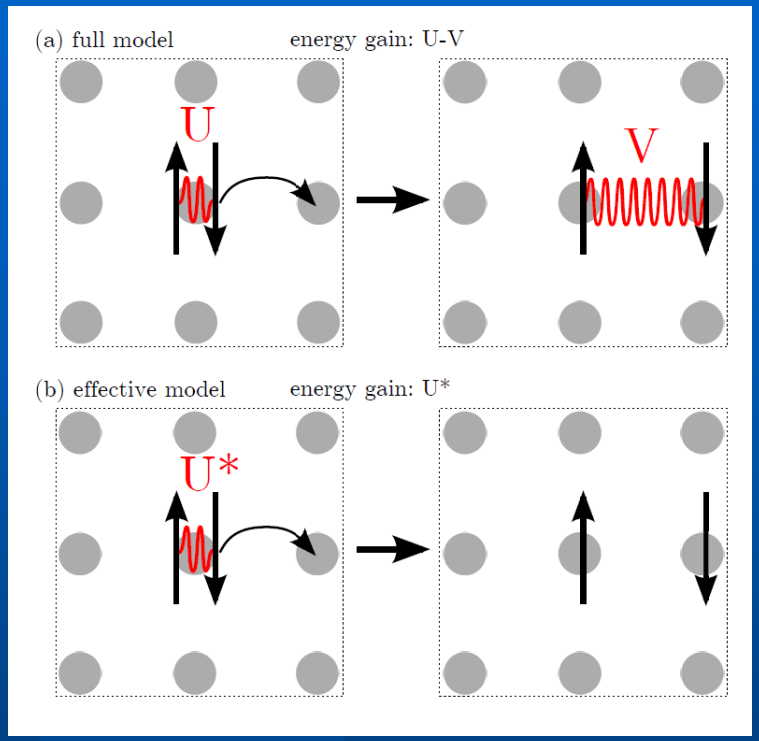

For translationally invariant system:

$$U^* = U - \bar{V}$$

$$\bar{V} = -\sum_{\substack{j\neq 0 \\ \sigma'}} V_{0j} \frac{\partial_{U^*} \langle n_{0\uparrow} n_{j\sigma'} \rangle^*}{\partial_{U^*} \langle n_{0\uparrow} n_{0\downarrow} \rangle^*}$$

Number of particle conservation

$$\sum_{j\sigma} \langle n_{0\uparrow} n_{j\sigma} \rangle^* = N/2$$

$$\partial_{U^*} \langle n_{0\uparrow} n_{0\downarrow} \rangle^* = -\sum_{j\neq 0,\sigma} \partial_{U^*} \langle n_{0\uparrow} n_{j\sigma} \rangle^*$$

A naive estimation: $U^* = U - V_{01}$

turns out to be amazingly good

Effective Hubbard model for graphene IV

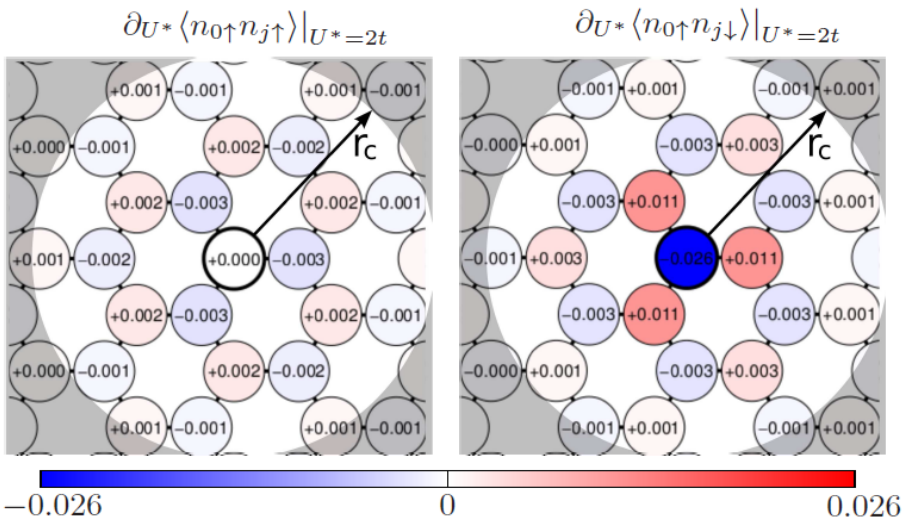

Figure 2. (Color online) Derivatives of the correlation functions $\langle n_{0\uparrow}n_{j\sigma}\rangle$ with respect to U^* for graphene (16x16 unit cells) calculated with DQMC for inverse temperature $\beta = 9t$ and $U = 2t$. Each circle corresponds to one carbon atom. The shaded area depicts the region of nearly vanishing derivatives. The cutoff radius is r_c. The thick drawn circles indicate the lattice site with index $i = 0$.

Calculations for benzene, graphene and silicene

Table I. First three rows: Coulomb matrix elements obtained with cRPA ($t_{\text{graphene}} = 2.80$ eV, $t_{\text{silicene}} = 1.14$ eV, $t_{\text{benzene}} = 2.54$ eV). Last three rows: Effective local Coulomb matrix elements with and without the approximation that electrons are only displaced to next neighbors and the factor by which the local Coulomb interaction is decreased.

	Graphene	Silicene	Benzene
U/t	3.63	4.19	3.96
$(V_{01},V_{02})/t$	2.03,1.45	2.31,1.72	2.83,2.01
$(V_{03},V_{04})/t$	1.32,1.14	1.55,1.42	1.80
U^*/t	1.6 ± 0.2	2.0 ± 0.3	1.2
$(U - V_{01})/t$	1.6	1.9	1.1
U^*/U	0.45 ± 0.05	0.46 ± 0.05	0.3

Decrease of effective *U* roughly by a factor of 2

Semimetal-insulator phase transition

M. Ulybyshev, P. Buividovich, MIK & M. Polikarpov, PRL111, 056801 (2013)

Lattice QMC simulations; Hubbard-Stratonovich transformation:

18 by 18 sites,
20 time slices,
T = 0.5 eV

(should be improved in future!)

$$\exp\left(-\frac{\delta}{2}\sum_{x,y}\hat{q}_x V_{xy}\hat{q}_y\right) \cong$$

$$\cong \int \mathcal{D}\varphi_x \exp\left(-\frac{\delta}{2}\sum_{x,y}\varphi_x V^{-1}_{xy}\varphi_y - i\delta\sum_x \varphi_x \hat{q}_x\right),$$

$$\mathrm{Tr}\, e^{-\beta\hat{H}} = \int \mathcal{D}\varphi_{x,n}\mathcal{D}\psi_{x,n}\mathcal{D}\eta_{x,n}\mathcal{D}\bar{\psi}_{x,n}\mathcal{D}\eta_{x,n}$$

$$e^{-S[\varphi_{x,n}] - \sum\limits_{x,y,n,n'}\left(\bar{\eta}_{x,n}\bar{M}_{x,y,n,n'}\eta_{y,n'} + \bar{\psi}_{x,n}M_{x,y,n,n'}\psi_{y,n'}\right)},$$

$$\mathrm{Tr}\, e^{-\beta\hat{H}} \cong \int \mathcal{D}\varphi_{x,n} e^{-S[\varphi_{x,n}]} |\det\left(M\left[\varphi_{x,n}\right]\right)|^2$$

Neutrality point: μ = 0

No sign problem (e-h symmetry)!

$$S\left[\varphi_{x,n}\right] = \frac{\delta}{2}\sum_{x,y,n}\varphi_{x,n}V^{-1}_{xy}\varphi_{y,n}$$

Semimetal-insulator phase transition II

The effect of screening by σ-bonds is essential. At our distances a factor 1.4

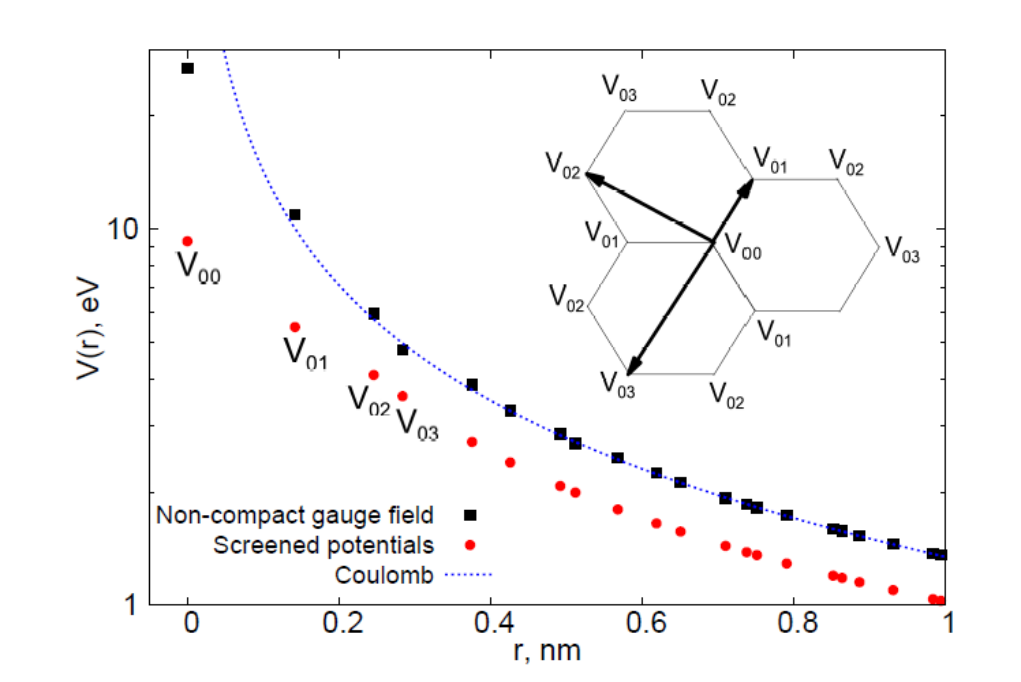

(1) Introduce the mass term *m*
(2) Chiral condensate Δ*n*, difference in occupation number between A and B sublattices
(3) Introduce external dielectric constant (due to substrate) ε

Semimetal-insulator phase transition III

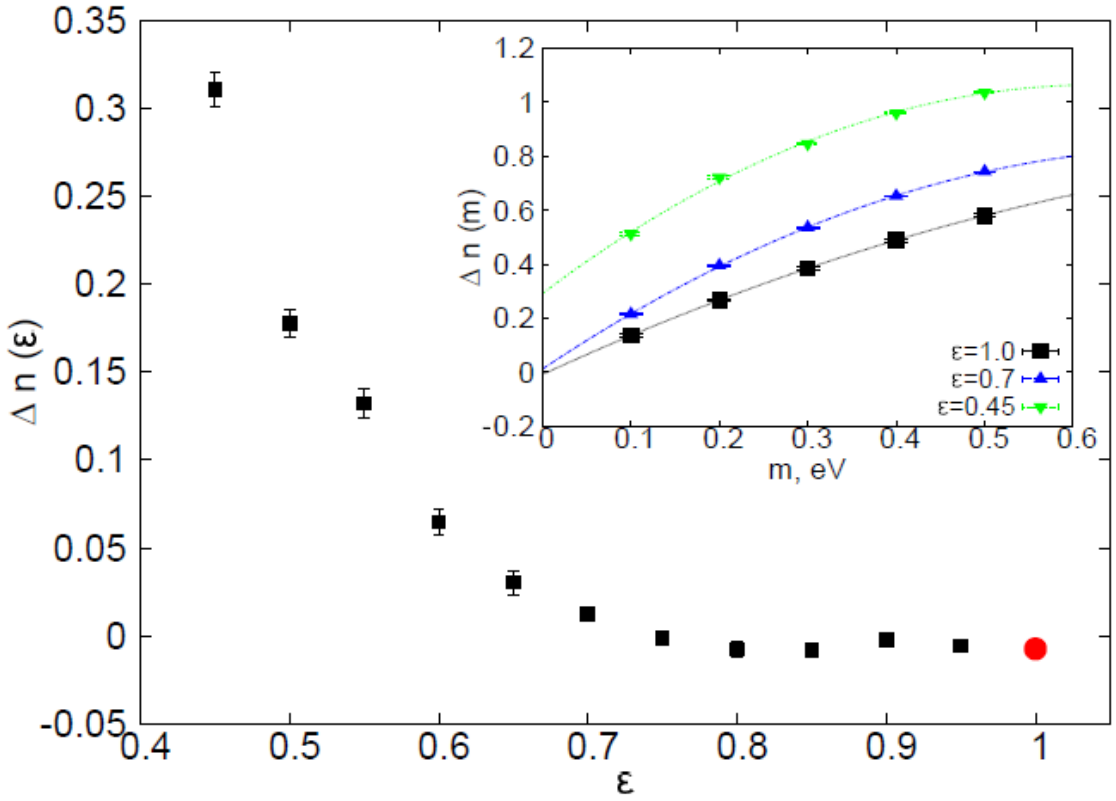

We are on semimetal side (screening by σ bonds is crucial) but not too far from the transition point $\varepsilon \approx 0.7$

Exciton fluctuations may be important

FIG. 2: The dependence of the chiral condensate (11) on ϵ and on m (in the inset) for the 18×18 lattice with $N_t = 20$ and $\delta = 0.1\,\mathrm{eV}^{-1}$. For $\epsilon = 1.0$ we show the results obtained on the 24×24 lattice with $N_t = 40$, $\delta = 0.05\,\mathrm{eV}^{-1}$.

Effect of vacancies/adatoms: QMC

M. Ulybyshev & MIK, PRL 114, 246801 (2015)

Random missing sites equally distributed in two sublattices

AFM state with very strong exchange interactions

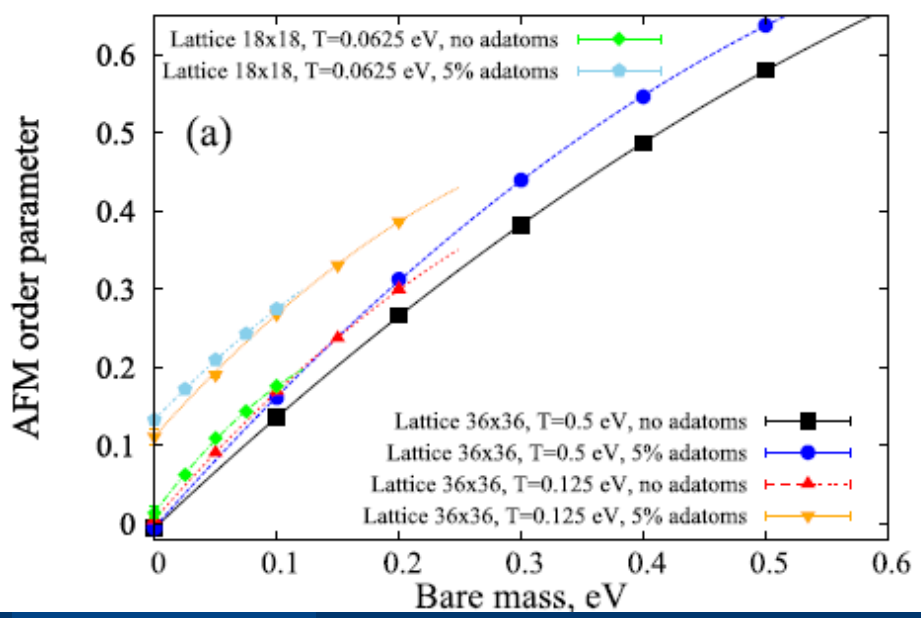

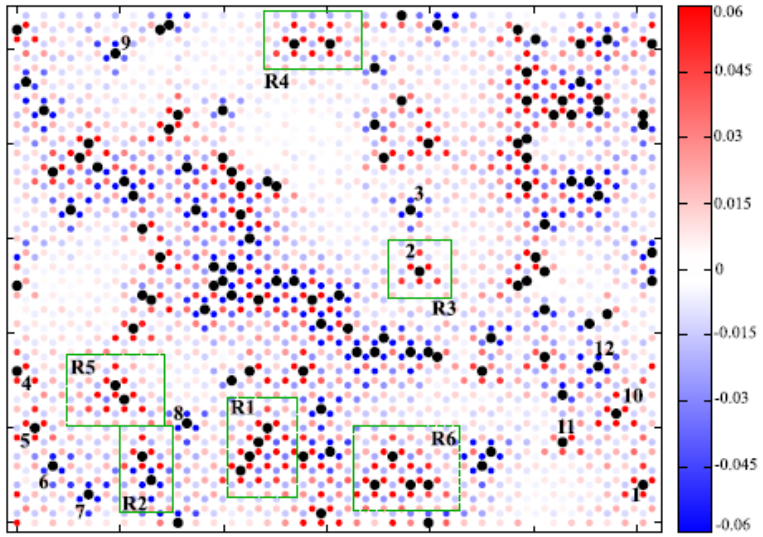

FIG. 2 (color online). Distribution of average spin. The color scale corresponds to $\langle S_z \rangle$ at a site in the zero bare mass limit.

Effect of vacancies/adatoms II

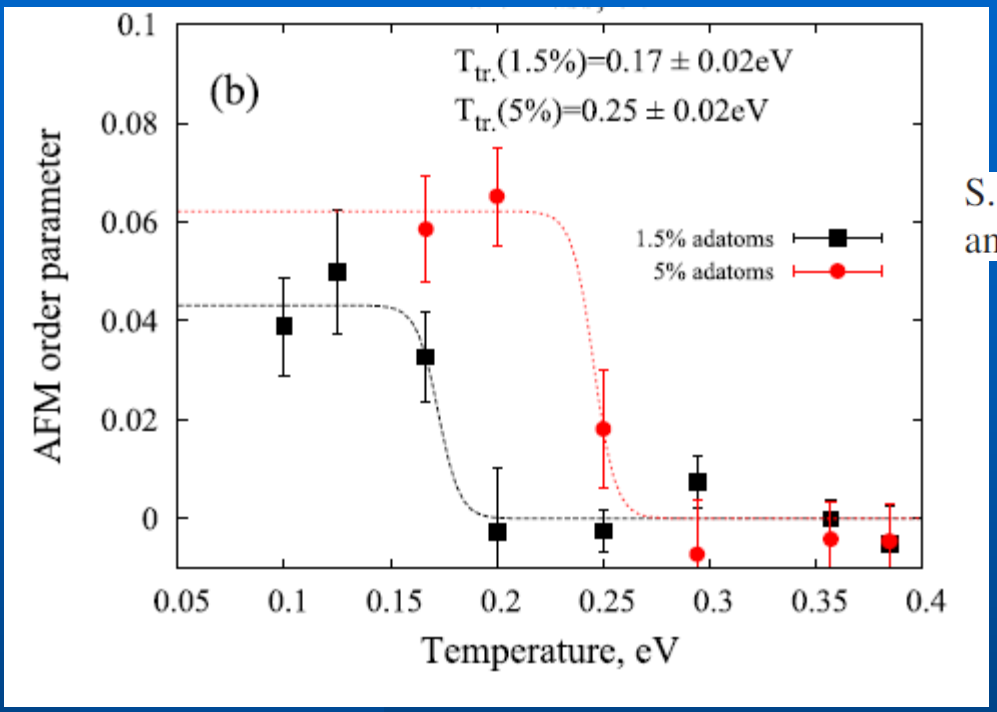

For vacancies: clearly contradict experiments

S. Just, S. Zimmermann, V. Kataev, B. Büchner, M. Pratzer, and M. Morgenstern, Phys. Rev. B **90**, 125449 (2014).

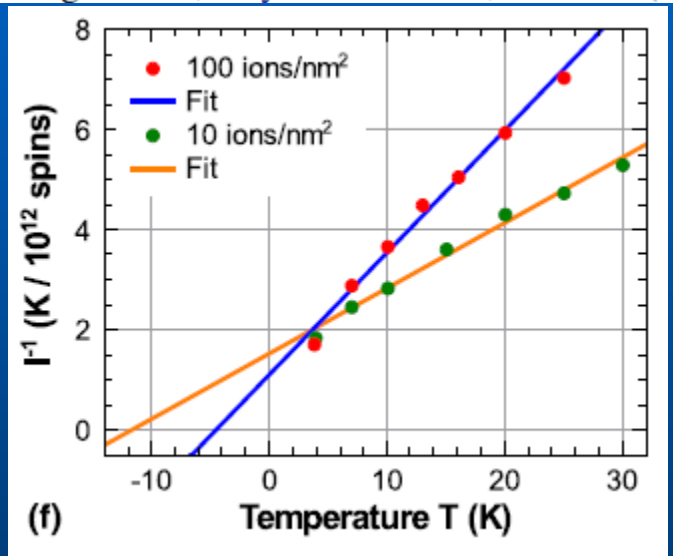

(f) Temperature-dependent inverse peak area of the ESR curves calibrated by a ruby standard (see text) in comparison with fit curves $a(T - \theta_{cw})$ revealing $\theta_{cw} = -12$ K and $\theta_{cw} = -5$ K, respectively.

Model of empty sites gives too srong antiferromagnetic exchange

Effect of vacancies/adatoms III

nature physics

LETTERS

PUBLISHED ONLINE: 10 JANUARY 2012 | DOI: 10.1038/NPHYS2183

Spin-half paramagnetism in graphene induced by point defects

R. R. Nair[1], M. Sepioni[1], I-Ling Tsai[1], O. Lehtinen[2], J. Keinonen[2], A. V. Krasheninnikov[2,3], T. Thomson[1], A. K. Geim[1] and I. V. Grigorieva[1]*

both scarce and controversial[13–16]. Here we show that point defects in graphene—(1) fluorine adatoms in concentrations x gradually increasing to stoichiometric fluorographene $CF_{x=1.0}$ (ref. 17) and (2) irradiation defects (vacancies)—carry magnetic moments with spin 1/2. Both types of defect lead to notable paramagnetism but no magnetic ordering could be detected down to liquid helium temperatures. The induced paramagnetism dominates graphene's low-temperature magnetic properties, despite the fact that the maximum response we could achieve was limited to one moment per approximately 1,000 carbon atoms. This limitation is explained by

For fluorinated graphene: mostly no local moments (or very high AFM coupling between them)

For vacancies: quite strong distortion, buckling etc., other rlectron states are involved

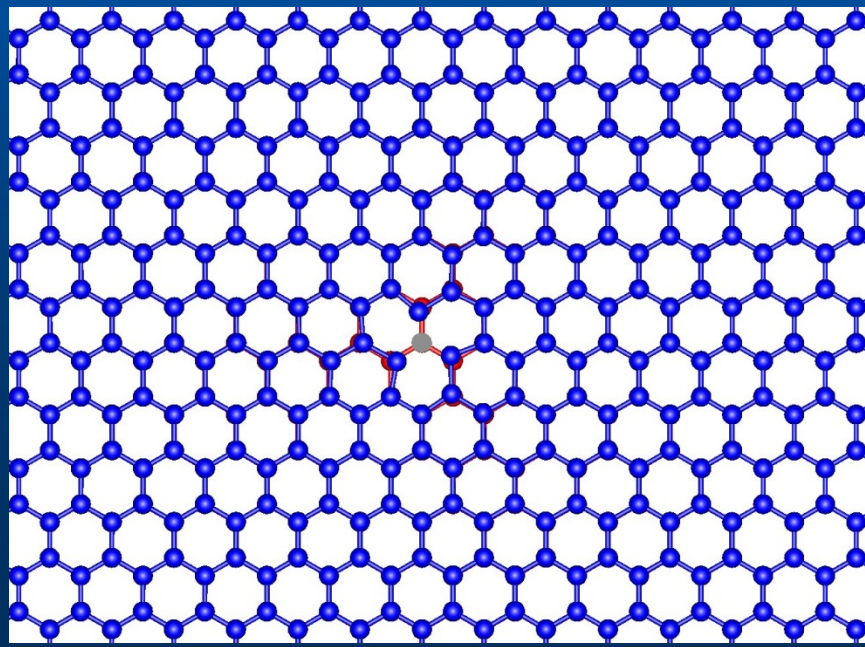

Effect of vacancies/adatoms IV

Gap opening dut to Coloumb interaction

	Center 1	Width 1	Center 2	Width 2	Gap
Ordinary potentials	0.76	0.40	-0.69	0.22	1.1 ± 0.17
Screened potentials	0.52	0.16	-0.49	0.18	0.74 ± 0.12

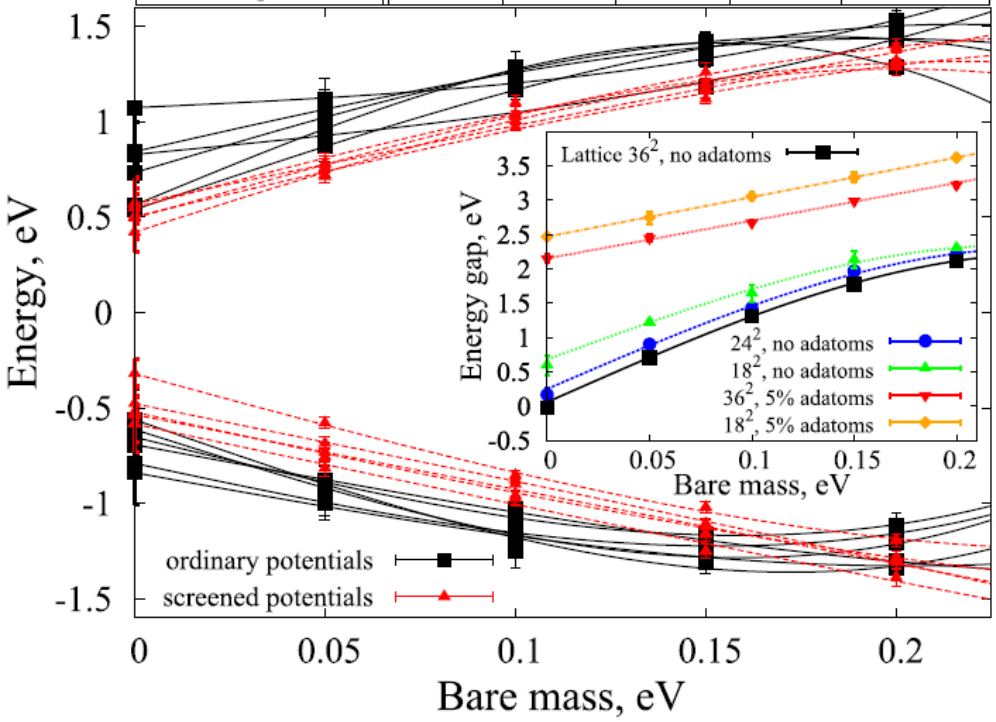

FIG. 3 (color online). Energies of the midgap states for two sets of interelectron potentials. Each state corresponds to one isolated vacancy marked with the number in Fig. 2. The center and width of the bands are calculated in the limit $m \to 0$. The center is the average over the energies of all states in each band and the width is equal to the doubled dispersion. $T = 0.125$ eV. The real physical situation is restored in the limit $m \to 0$. Inset: energy gap between normal energy bands. All values correspond to the K point in the Brillouin zone.

Quite noticeable gap in impurity band and much larger in K point for freely suspended graphene with 5% defects.

Can be measured optically

Renormalization of Fermi velocity

Coulomb interaction of 2D masless fermions
(Gonzales, Guinea, Vozmediano, Nucl. Phys. B 1994)
Zero doping (Fermi level at the Dirac point)
Logarithmic renormalization of the Fermi velocity due to Fock contribution

$$\hat{H}_F = \sum_{\vec{k}} \sum_{\alpha,\chi} \hat{\psi}_\alpha^{+}\left(\vec{k}\right) h_{\alpha\beta}\left(\vec{k}\right) \hat{\psi}_\beta\left(\vec{k}\right)$$

$$h_{\alpha\beta}\left(\vec{k}\right) = -2\pi e^2 \sum_{\vec{k}'} \frac{\rho_{\beta\alpha}\left(\vec{k}'\right)}{\left|\vec{k}-\vec{k}'\right|}$$

$$\rho_{\beta\alpha}\left(\vec{k}\right) = \left\langle \hat{\psi}_{\vec{k}\alpha}^{+} \hat{\psi}_{\vec{k}\beta} \right\rangle$$

$$\delta v_F = \frac{e^2}{4\hbar} \ln\left(\frac{\Lambda}{k_F}\right)$$

$\Lambda \propto 1/a$ is the ultraviolet cut-off due to inapplicability of Dirac model at large wave vectors

Renormalization of Fermi velocity II

PHYSICAL REVIEW B **92**, 245105 (2015)

Many-body effects in graphene beyond the Dirac model with Coulomb interaction

N. Yu. Astrakhantsev,[1,2,*] V. V. Braguta,[3,4,5] and M. I. Katsnelson[6,7]

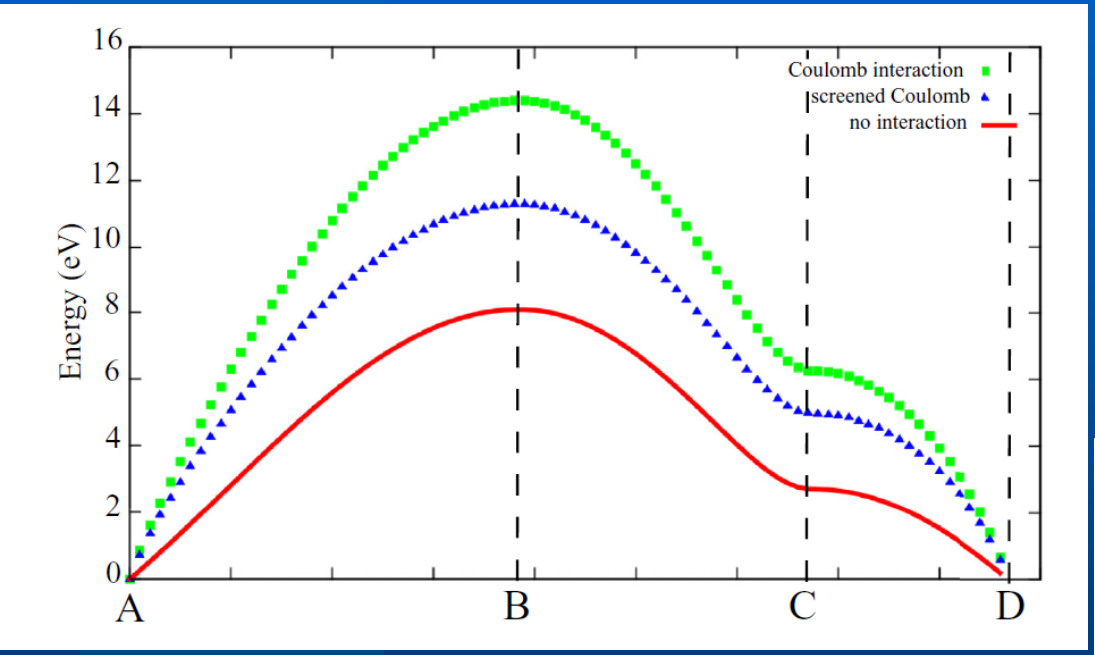

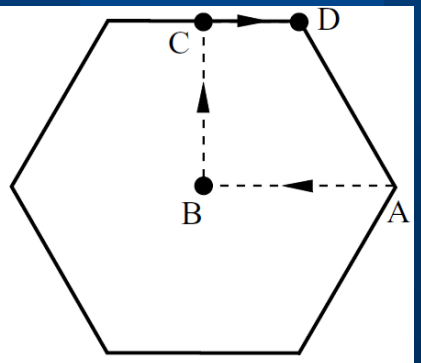

Effect of screening is quite important

Graphene on hBN, Coulomb interaction

$$v_F^R(T)/v_F^0 = \left(1 + A \log\left[\frac{\Lambda}{\mu}\right]\right)$$

$$A = 0.096,\ \Lambda = 3.2\ \text{eV}$$

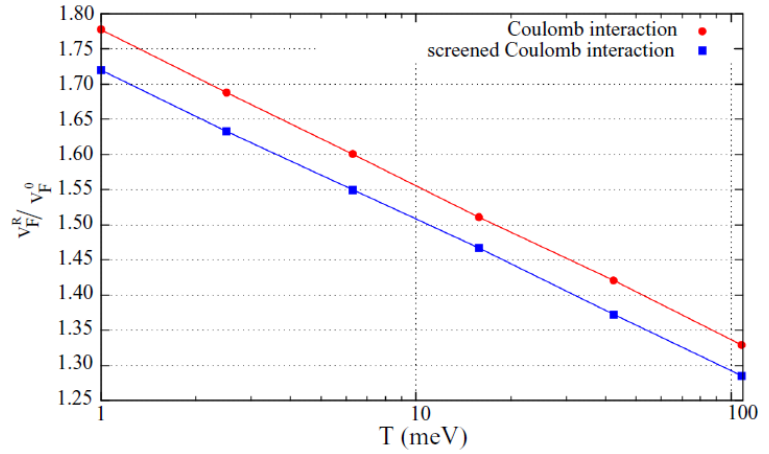

FIG. 11. (Color online) The renormalization factor for the Fermi velocity as a function of the temperature for graphene on hBN for Coulomb and screened at small distance Coulomb interactions [23].

Renormalization of Fermi velocity III

Seen in Schibnikov-de Haas (Elias et al, Nature Phys. 2011) and quantum capacitance (Yu et al, PNAS 2013) exper.

$$1/C = 1/C_G + 1/C_Q$$

$$C_Q = Se^2\, dn/d\mu$$

Fitting

$$v_F(\mu) = v_F(\mu_0)\left(1 + \frac{1}{4}\frac{\alpha}{\epsilon(v_F/c)}\log\left[\frac{\mu_0}{\mu}\right]\right)$$
$$= v_F(\mu_0)\left(1 + A\log\left[\frac{\mu_0}{\mu}\right]\right),$$

$$v_F(\mu_0) = 0.85 \times 10^6 \text{ m/s}, \quad \mu_0 = 3.2 \text{ eV}$$

$$\epsilon \simeq 8, \text{ and } A = 0.081$$

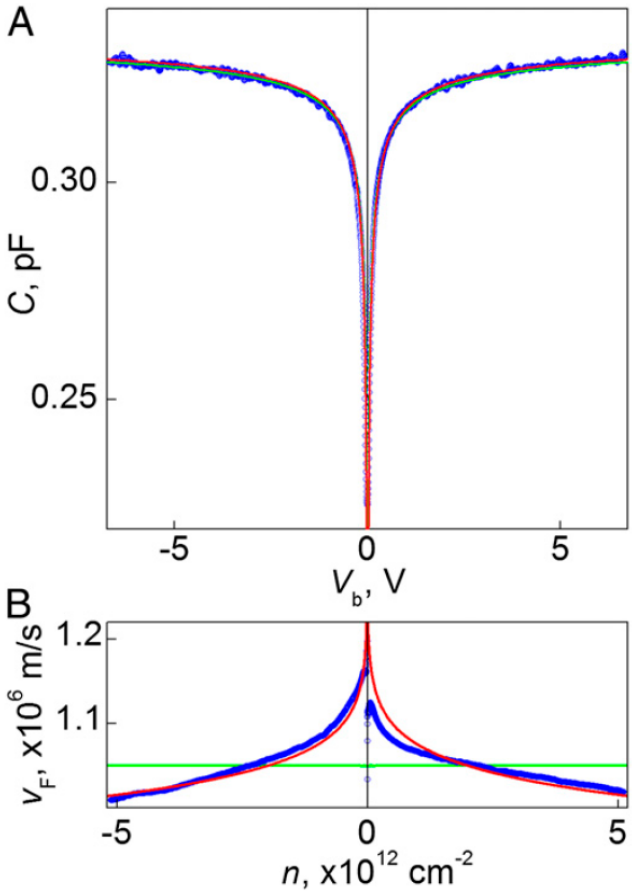

Fig. 2. Quantum capacitance of graphene. (*A*) Differential capacitance in zero *B*. Blue symbols are experimental data; green and red curves are the best fits with constant and renormalized v_F, respectively. This particular device has $d \sim 27$ nm and $S \sim 250$ μm^2. (*B*) Same data replotted in terms of v_F and carrier concentration n; color coding as in *A*.

Optics

Single-particle result for the Dirac Fermions:

$$\text{absorption } P = W_a/W_i = \pi e^2/\hbar c = \pi\alpha$$

Experiment:

Fine Structure Constant Defines Visual Transparency of Graphene

R. R. Nair,[1] P. Blake,[1] A. N. Grigorenko,[1] K. S. Novoselov,[1] T. J. Booth,[1] T. Stauber,[2] N. M. R. Peres,[2] A. K. Geim[1]*

6 JUNE 2008 VOL 320 SCIENCE

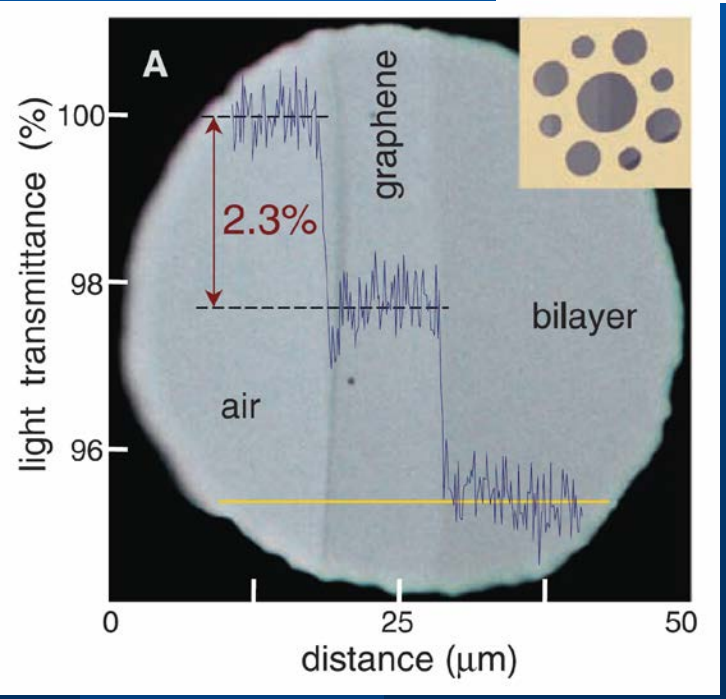

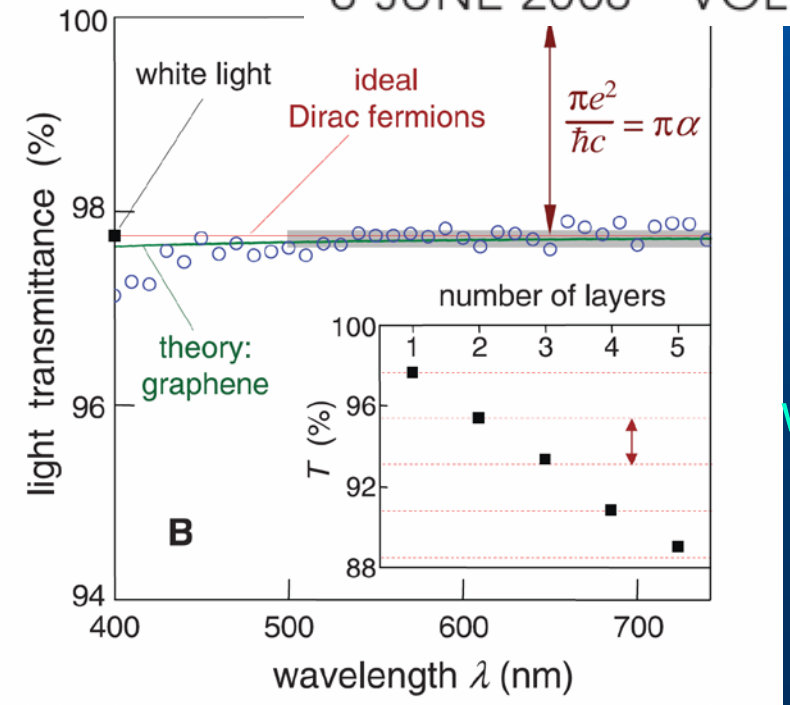

No corrections within accuracy 3%

Optics II

Do we expect renormalization? A controversial issue

For short-range interaction one expects no renormalization

Phenomelonogical theory of Fermi liquid:

M. I. Katsnelson, Europhys. Lett. **84**, 37001 (2008)

Microscopic theory for Hubbard model:

A. Giuliani, V. Mastropietro, and M. Porta, Phys. Rev. B **83**, 195401 (2011).

For Coulomb interaction graphene is not Fermi liquid

α_{eff} logarithmically dependent on frequency

$$\frac{\sigma(\omega)}{\sigma_0} = 1 + C\alpha_{\text{eff}} + O\left(\alpha_{\text{eff}}^2\right)$$

Various ways of regularization gives C = 0.01, or C=0.26

Optics III

Lattice QMC

PHYSICAL REVIEW B **94**, 085421 (2016)

Many-body effects on graphene conductivity: Quantum Monte Carlo calculations

D. L. Boyda,[1,2,*] V. V. Braguta,[2,3,4,†] M. I. Katsnelson,[5,6,‡] and M. V. Ulybyshev[7,8,§]

Numerically: almost no renormalization in semimetal phase and strong renormalization in AFM insulator phase

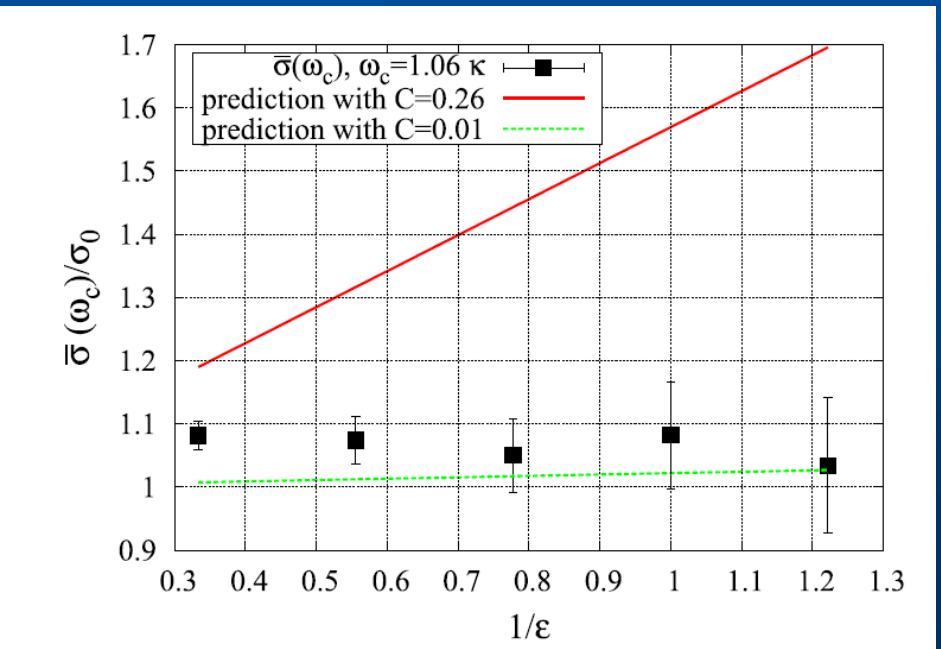

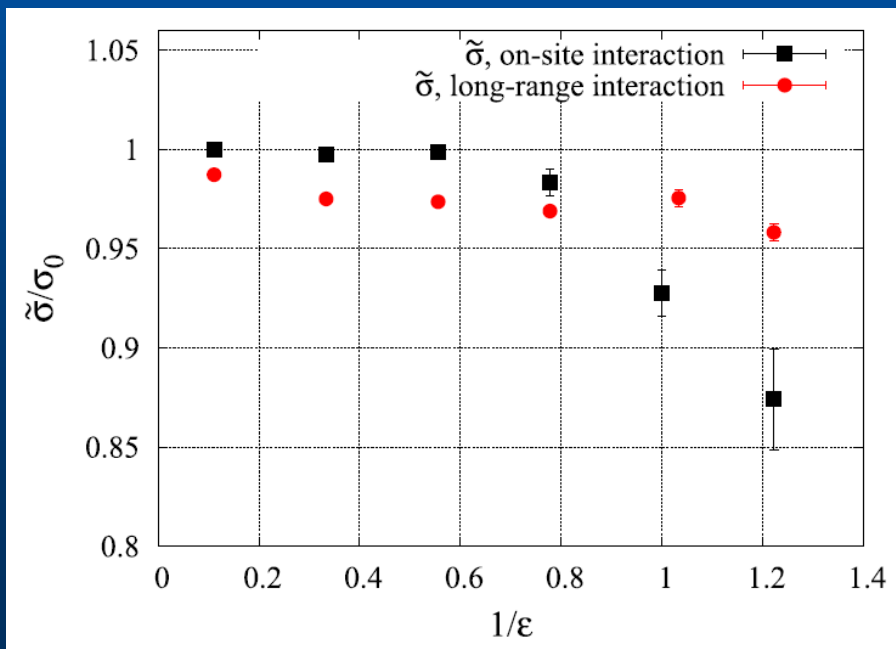

Static screening

PHYSICAL REVIEW B **97**, 035102 (2018)

Quantum Monte Carlo study of electrostatic potential in graphene

N. Yu. Astrakhantsev,[1,2,*] V. V. Braguta,[1,2,4,5,†] M. I. Katsnelson,[6,7] A. A. Nikolaev,[1,3] and M. V. Ulybyshev[8]

RPA (lowest order) result:

$$\epsilon = 1 + \frac{\pi}{2}\alpha_{\text{eff}}$$

$$\alpha_{\text{eff}} = \alpha \cdot c/v_F \sim 300/137 \sim 2.2$$

No small parameters, how good is it?

Second-order result:

$$\epsilon = 1 + \frac{\pi}{2}\alpha_{\text{eff}} + 0.778\alpha_{\text{eff}}^2$$

I. Sodemann and M. M. Fogler, Phys. Rev. B **86**, 115408 (2012).

Corrections are significant!

Static screening II

Monte Carlo simulations: put two point charges, calculate effective interaction energy,

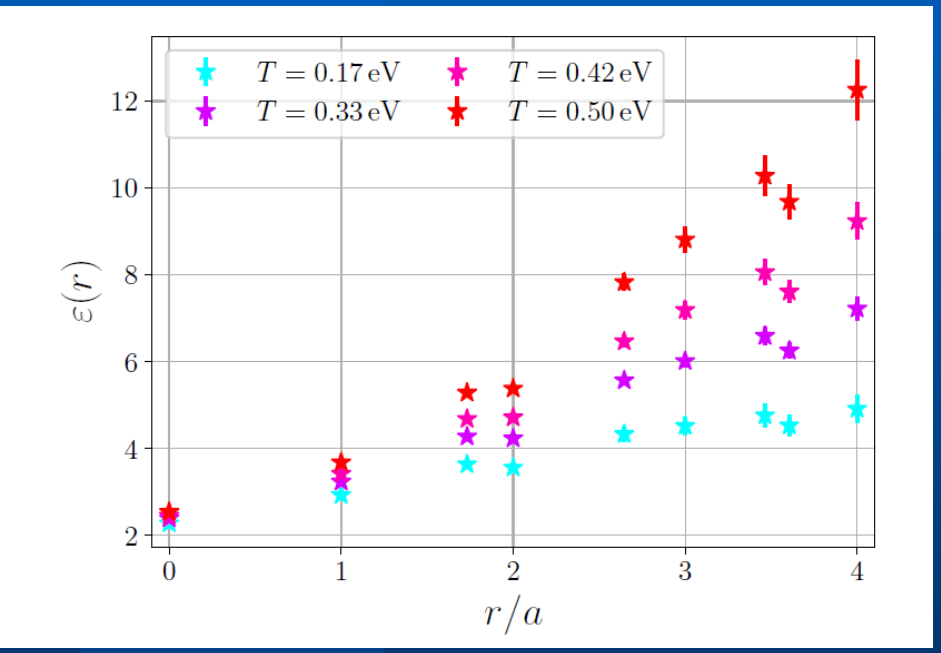

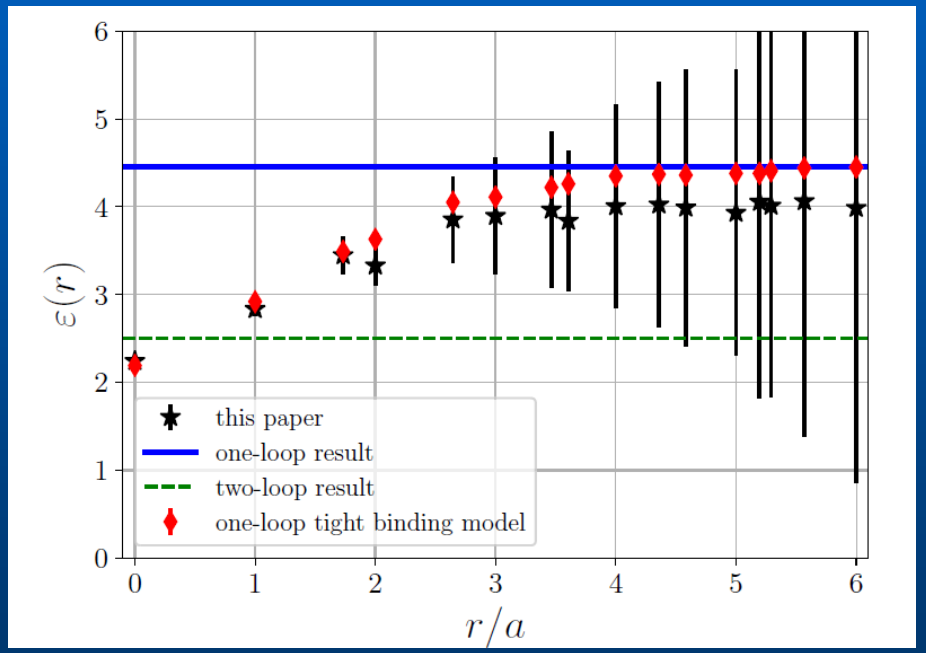

Zero-temperature results

Static screening III

Perturbative (RPA) result fits very well the QMC despite of the absence of any explicit small parameter

r/a	$\varepsilon(r)$	$\varepsilon_{1\,\mathrm{loop}}(r)$
0.00	2.24 ± 0.02	2.19
1.00	2.83 ± 0.08	2.92
1.73	3.45 ± 0.21	3.49
2.00	3.33 ± 0.23	3.63
2.65	3.86 ± 0.49	4.05
3.00	3.89 ± 0.66	4.11
3.46	3.97 ± 0.88	4.22
3.61	3.84 ± 0.80	4.26
4.00	4.01 ± 1.15	4.35

Quantum-Limited Resistivity

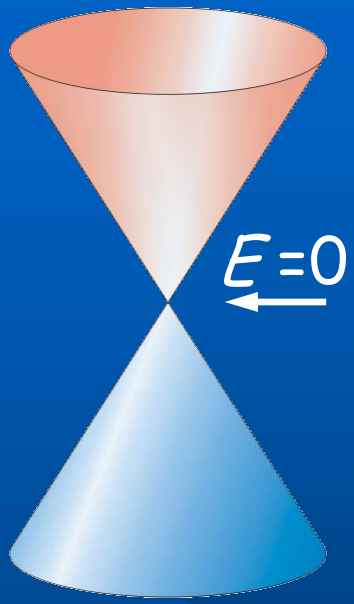

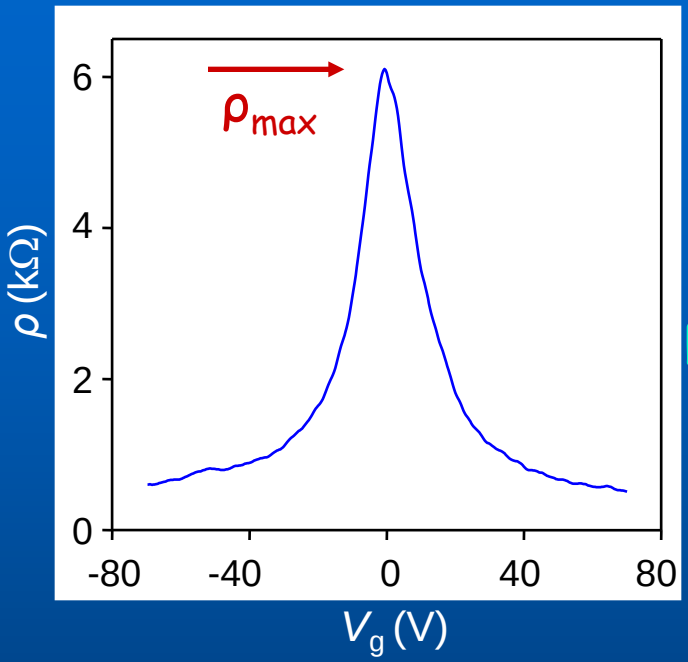

no temperature dependence in the peak between 3 and 80K

zero-gap semiconductor

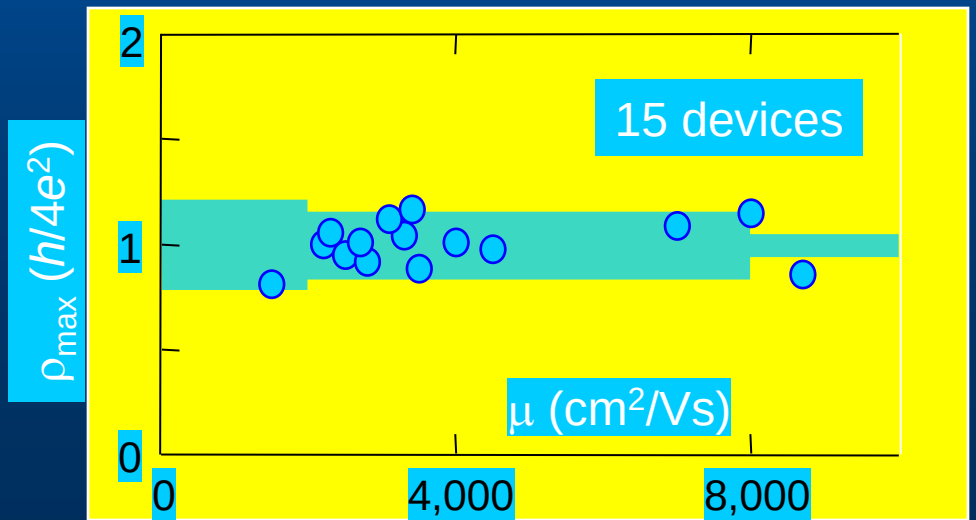

Novoselov et al, Nature 2005

Transport via evanescent waves

MIK, EPJ B 51, 157 (2006)

Conductance = e^2/h *Tr T* per valley per spin

T is the transmission probability matrix

The wave functions of massless Dirac fermions at zero energy:

$$\left(\frac{\partial}{\partial x} \pm i\frac{\partial}{\partial y}\right)\psi_{\pm}(x,y) = 0 \qquad \psi_{\pm}(x,y) = f(x \pm iy) \qquad \forall f$$

Boundary conditions determine the functions *f*

Transport via evanescent waves II

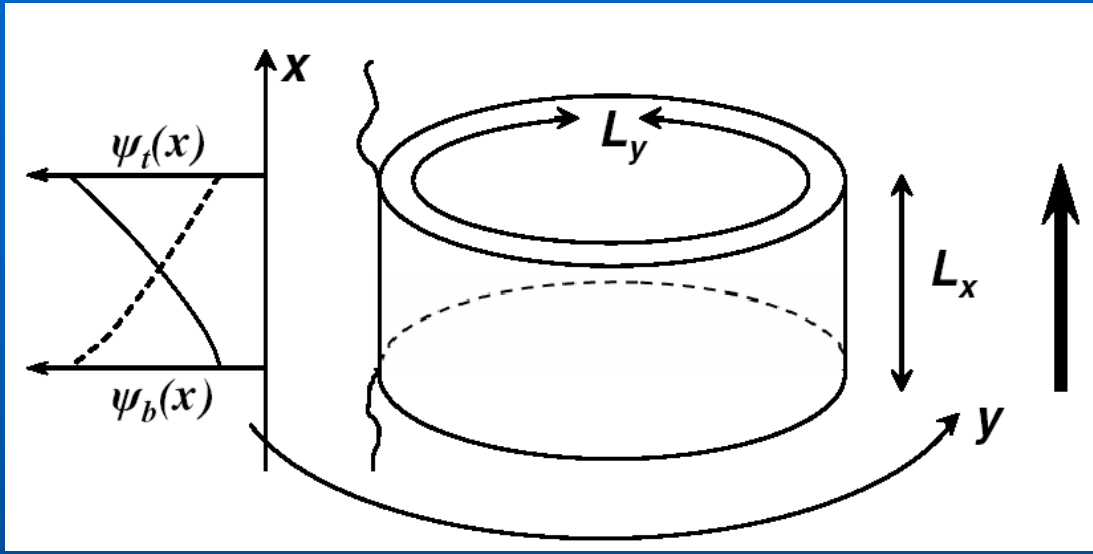

$$\psi_{\pm}(x,y) = \exp\left[\frac{2\pi n}{L_y}(x \pm iy)\right] \qquad n = 0, \pm 1, \pm 2, \ldots$$

$f(y+L_y) = f(y)$ Edge states near the top and bottom of the sample

New type of electron transport: via evanescent waves – different from both ballistic and diffusive

Transport via evanescent waves III

Leads from doped graphene

$$T_n = |t(k_y)|^2 = \frac{\cos^2\phi}{\cosh^2(k_y L_x) - \sin^2\phi}$$

$$\sin\phi = k_y / k_F$$

$$TrT = \sum_{n=-\infty}^{\infty} \frac{1}{\cosh^2(k_y L_x)} \simeq \frac{L_y}{\pi L_x}$$

Conductivity per channel: $e^2/(\pi h)$

The problem of “missing pi(e)” – may be, no problem

Many-body renormalization

F. Guinea & MIK, PRL 112, 116604 (2014)

Caldeira & Leggett, 1981, 1983: tunneling with dissipation

Overlap of the wave functions are suppresed by overlap of the wave functions of environment (then, averaging over the environment)

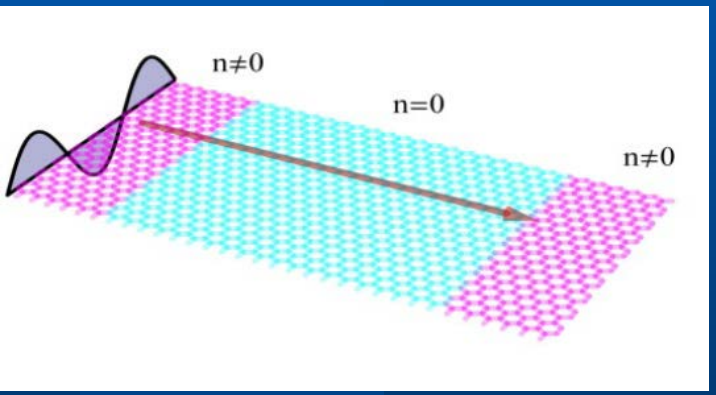

Transport via evanescent waves is tunneling

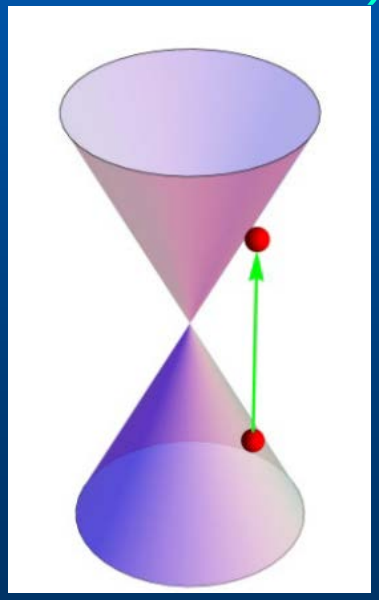

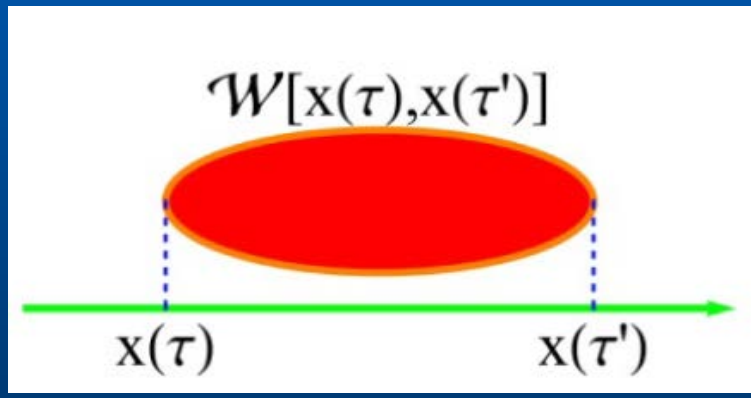

Nonlocal self-interaction

e-h pairs as thermal bath

Many-body renormalization II

Correction to the effective tunneling action

$$\delta S = \frac{1}{2}\int_{-\infty}^{+\infty} d\tau \int_0^{\beta} d\tau' \int_{-\infty}^{+\infty} \frac{dq}{2\pi} \int_{-\infty}^{+\infty} d\omega \, e^{iq[x(\tau)-x(\tau')-\omega|\tau-\tau'|]} W(q,\omega)$$

Screened Coulomb interaction

$$W(q,\omega) = \frac{v_q}{\epsilon(q,\omega)}$$

Bare Coulomb interaction

$$v_q \simeq \begin{cases} -\frac{2e^2}{\epsilon_0}\log(qL_y) & qL_y \ll 1 \\ \frac{2\pi e^2}{\epsilon_0 q L_y} & 1 \ll qL_y \end{cases}$$

For undoped graphene

$$\epsilon(q,\omega) = 1 + v_q \chi_{1D}(q,\omega)$$

$$\chi_{1D}(q,\omega) \approx L_y \chi_{2D}(q,\omega) \approx L_y \frac{q^2}{4\sqrt{v_F^2 q^2 - \omega^2}}$$

Many-body interaction III

Suppression of tunneling probability

$$T(k_y) \cong T_0(k_y) e^{-\delta S}$$

$$\delta S_G \approx \frac{L_x}{8\pi L_y} \frac{\alpha^2}{4\sqrt{2}+\alpha} \log\left(\frac{L_x}{a}\right)$$

for isolated graphene

In the presence of metallic layer:

$$g = k_F \ell$$

$$\chi_{1D}^{M}(q,\omega) \approx \begin{cases} \frac{v_{1D} D q^2}{i\omega + D q^2} & q \le \ell^{-1} \\ \frac{v_{1D} v_F^M q}{i\omega + v_F^M q} & \ell^{-1} \le q \le k_F \end{cases}$$

$$\delta S_M = \delta S_d + \delta S_b \approx \frac{L_x^2}{4\pi g \ell L_y} + \frac{L_x}{8\pi L_y} \log(g)$$

Many-body renormalization IV

At finite temperatures the cut-off wave vector

$$q_c \approx \mathrm{Max}(L_x^{-1}, T/\mathrm{v}_F)$$

Magnetic field effects on diffusion!

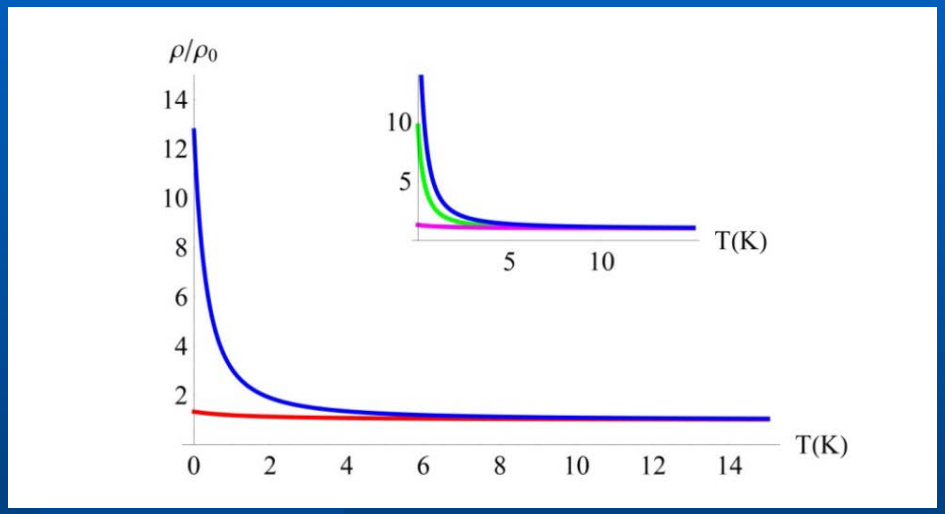

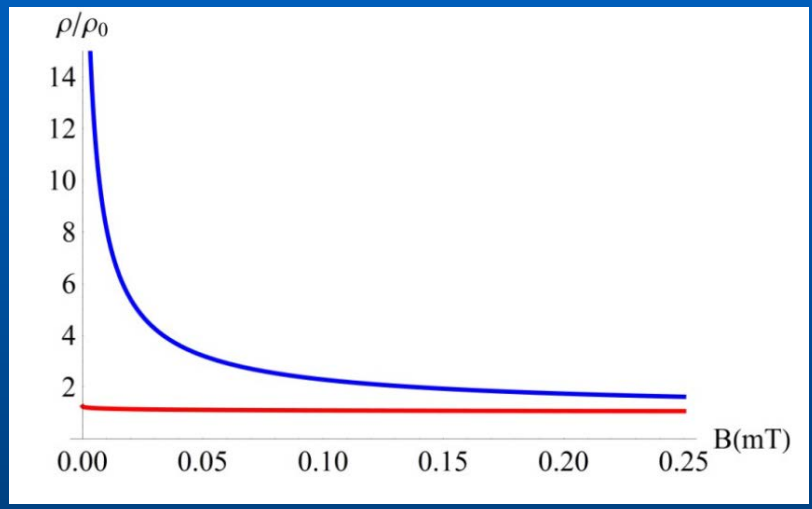

FIG. 2. Temperature dependence of the inverse conductance, normalized to the non interaction value, $\sigma_0 = e^2/(\pi\hbar)$, for $L_x = 4\mu$, $L_y = 1\mu$. Red: Contribution from the graphene excitations, δS_G, eq. 6. Blue: Contribution from a metallic layer, δS_M, eq. 8. The two terms which describe the contribution from the metal, δS_d and δS_b are shown in the inset. Green: diffusive part, δS_d in eq. 8. Magenta: ballistic part, δS_b in eq. 8. The carrier density in the metal is $n = 10^{11}\mathrm{cm}^{-1}$, and the elastic mean free path is $\ell = 100\mathrm{nm}$.

T= 1K

A recent experiment

PRL 110, 216601 (2013) PHYSICAL REVIEW LETTERS week ending 24 MAY 2013

Insulating Behavior at the Neutrality Point in Single-Layer Graphene

F. Amet,[1] J. R. Williams,[2] K. Watanabe,[3] T. Taniguchi,[3] and D. Goldhaber-Gordon[2]

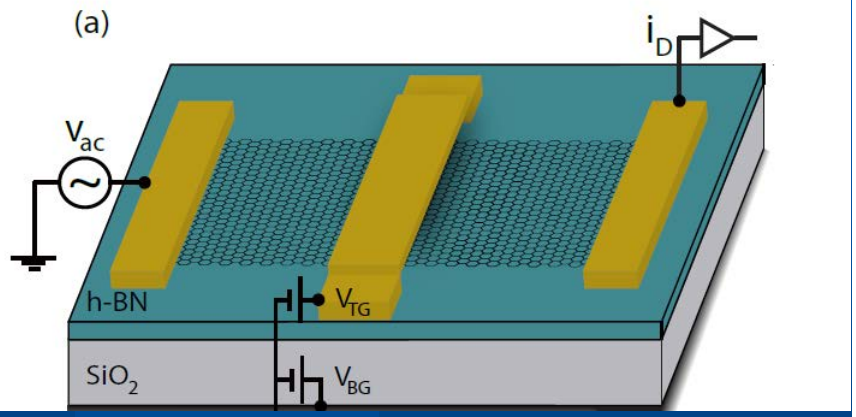

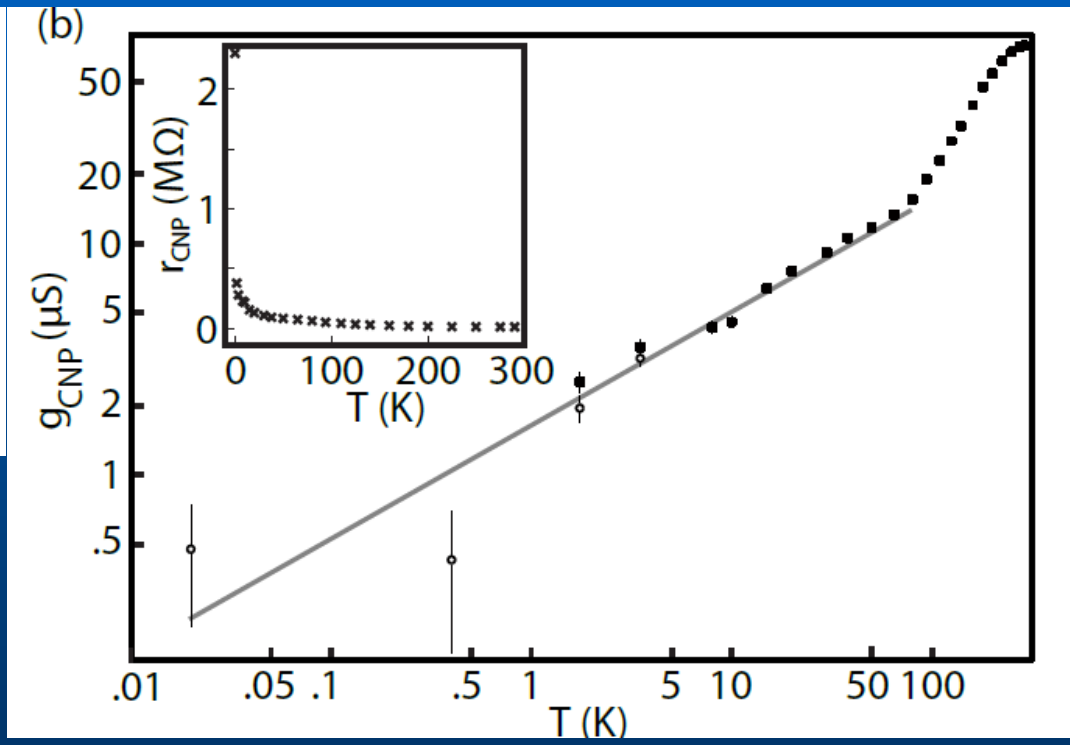

Also, graphene on hBN

Power-law behavior with temperature

$$g_{CNP} \propto T^{\alpha} \text{ with } \alpha \approx 0.48 \pm 0.05$$

Conclusions

Nonlocal interaction, no small parameters, still a lot of open questions

Main collaborators

A.Geim, K.Novoselov (Manchester)
F.Guinea (Madrid & Manchester)
A.Lichtenstein (Hamburg)
T.Wehling (Bremen)
M.Ulybyshev (Regensburg)
V.Braguta, N. Astrakhantsev (Moscow)

MANY THANKS!